Polarization of Σ^- in the Reaction $\pi^-+p \rightarrow \Sigma^-+K^+$ at 1130 MeV/c

J. A. EDGINGTON, V. J. HOWARD, M. C. MILLER, AND R. J. OTT
Queen Mary College, London, England

AND

P. J. DUKE, R. E. HILL, W. R. HOLLEY, D. P. JONES, AND J. J. THRESHER
Rutherford High Energy Laboratory, Chilton, Didcot, Berkshire, England

AND

J. C. SLEEMAN
Oxford University, Oxford, England
(Received 30 September 1968)

We have measured the polarization P_{Σ^-} of the Σ^- in the production reaction $\pi^-+p \rightarrow \Sigma^-+K^+$ due to a π^- beam of momentum 1130 MeV/c striking a polarized proton target. We find P_{Σ^-} to lie between -0.1 and -0.5 in each of seven angular bins in the range $-1.0<\cos\theta_\Sigma^*<0.3$. Combining this and other measurements, we have performed an energy-dependent partial-wave analysis of the associated production reactions $\pi p \rightarrow \Sigma K$ between threshold and 1170 MeV/c, using only S and P waves below 1130 MeV/c but including D waves at higher momenta. Using a momentum-dependent form for the amplitudes first proposed by Lee *et al.*, we find the $I=\frac{3}{2}$ amplitudes to be uniquely determined over the whole energy range, but the $I=\frac{1}{2}$ amplitudes to have several solutions of similar, but low, likelihood. Thus, this particular parametrization does not appear to hold for the $I=\frac{1}{2}$ channels near threshold. A possible reason is the presence of a highly inelastic P_{11} resonance in the direct channel.

I. INTRODUCTION

RECENTLY, several measurements have been reported of the cross sections and polarizations in the associated production reactions $\pi p \rightarrow \Sigma K$ in the π-momentum region between threshold and about 1200 MeV/c. Specifically, both sets of quantities have been quite well determined (see Table IV and references therein) for the channels Σ^+K^+ and Σ^0K^0, but only a single polarization measurement has been made in the channel Σ^-K^+, in one angular region and at an incident momentum of 1145 MeV/c.[1] A difficulty in measuring this quantity is that the asymmetry parameter α in the normal decay mode $\Sigma^- \rightarrow n\pi^-$ is close to zero,[2] making analyses of the Σ^- polarization, by studying its decay angular distribution, almost impossible. Partial-wave analyses[2-4] of these distributions have shown that waves with $l=0$ and 1 are adequate to describe the Σ^0K^0 and Σ^-K^+ channels up to 1200 MeV/c, but that the Σ^+K^+ results require orbital angular momenta up to $l=3$ at the higher energies. Fits to this latter channel have been used to obtain the pure $I=\frac{3}{2}$ production amplitudes.[3]

We report here a determination of the Σ^- polarization in the production reaction

$$\pi^-+p \rightarrow \Sigma^-+K^+ \qquad (1)$$

initiated by a π^- beam of momentum 1130 MeV/c striking a polarized proton target at the Nimrod proton synchrotron. We detected only the K^+ in the final state. The incident momentum was thus chosen as being below the threshold (1290 MeV/c) for production of the three-body final state $\Sigma^-K^+\pi^0$, and yet far enough above the Σ^-K^+ threshold (1040 MeV/c) for its cross section to be varying only slowly with energy. The angular asymmetry of the K^+ was measured by counter techniques over the range $-1.0<\cos\theta_\Sigma<0.3$ in the c.m. system. If we assume the $KN\Sigma$ relative parity to be odd[5,6] and define positive Σ^- polarization to be in the direction $\hat{k}_\pi \times \hat{k}_\Sigma$ (where k_π and k_Σ are the momenta of the π and Σ, respectively) we find a negative polarization of between -0.1 and -0.5 in each of seven angular bins. We find that partial waves up to and including $l=2$ are necessary to produce a good fit to our data. Combinding these and other measurements, we have performed an energy-dependent partial-wave analysis between threshold and 1170 MeV/c, obtaining values of the $I=\frac{1}{2}$ and $I=\frac{3}{2}$ production amplitudes for the reactions $\pi p \rightarrow \Sigma K$.

In Sec. II we discuss the principle of the measurement and give experimental details. Then we describe the data analysis and present the results; finally we discuss the partial-wave analysis.

II. EXPERIMENTAL METHOD

The beam line is shown in Fig. 1. It was an extension of an existing beam line derived from an internal copper

[1] D. Weldon, H. Steiner, G. Shapiro, C. Schultz, C. H. Johnson, Jr., L. Holloway, M. Hansroul, P. D. Grannis, B. Dieterle, O. Chamberlain, and J. Arens, Phys. Rev. **167**, 1199 (1968).
[2] J. C. Doyle, F. S. Crawford, Jr., and J. A. Anderson, Phys. Rev. **165**, 1483 (1968).
[3] F. S. Crawford, Jr., F. Grard, and G. A. Smith, Phys. Rev. **128**, 368 (1962).
[4] J. A. Anderson, F. S. Crawford, Jr., and J. C. Doyle, Phys. Rev. **152**, 1139 (1966).
[5] M. Watson, M. Ferro-Luzzi, and R. D. Tripp, Phys. Rev. **131**, 2248 (1963).
[6] B. D. Dieterle, J. F. Arens, O. Chamberlain, P. D. Grannis, M. J. Hansroul, L. E. Holloway, C. H. Johnson, Jr., C. Schultz, H. Steiner, G. Shapiro, and D. Weldon, Phys. Rev. **167**, 1190 (1968).

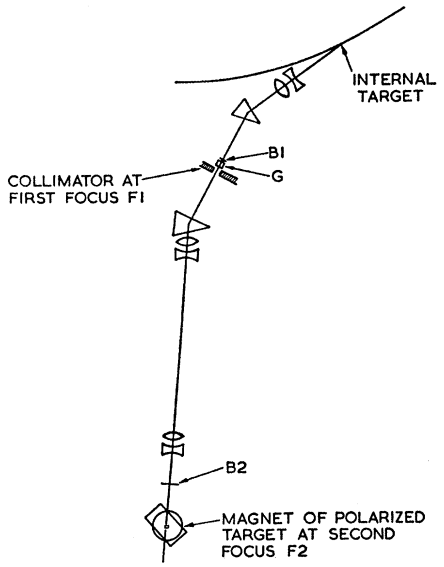

FIG. 1. Beam-transport system. The focusing directions of the quadrupole magnets refer to the horizontal plane.

target. A collimator at the first focus $F1$ restricted the momentum bite to approximately $2\frac{1}{2}\%$ full width at half maximum. At the second focus $F2$ the beam had full widths at half maximum of 1.75 cm vertically and 4.45 cm horizontally.

A polarized-proton target, whose construction and operation has been described in detail elsewhere,[7] was an assembly of crystals of neodymium-doped lanthanum magnesium nitrate (LMN). Each crystal was a regular octagon of side 1.05 cm and thickness 0.54 cm. Four of these were clamped together with spacers to allow the circulation of liquid helium, forming a target assembly 2.54-cm thick. The axis of eightfold symmetry was oriented along the beam direction. This assembly was placed in a vertical magnetic field of 18.6 kOe, which was perpendicular to the $\Sigma^- K^+$ production plane, i.e., to the direction $\hat{k}_\pi \times \hat{k}_\Sigma$, and was cooled to below 1.2°K using a horizontal continuous-flow helium cryostat. The spin directions of the free protons in the water of crystallization of the LMN could be oriented parallel or antiparallel to the field direction, by microwave pumping using the method of dynamic nuclear orientation[8]; the direction of polarization could be reversed by a small change in frequency. The magnitude of polarization was determined by NMR measurements; during the experiment it varied between about 0.4 and 0.6, with an average of 0.50 ± 0.08. Most of the error on this number arose from the absolute calibration of the NMR system performed under thermal-equilibrium conditions at 1.2°K. The polarization thus determined agrees with the value deduced from the asymmetry in $\pi^- p$ elastic scattering which was measured concurrently.

[7] H. H. Atkinson, *Proceedings of the International Conference on Polarized Targets and Ion Sources* (Saclay, 1966), p. 41.
[8] D. C. Jeffries, *Dynamic Nuclear Orientation* (Interscience Publishers, Inc., New York, 1963).

The experiment consisted of a measurement of the K^+ asymmetry ϵ given by

$$\epsilon(\theta) = [N_H{}^+(\theta) - N_H{}^-(\theta)]/[N_H{}^+(\theta) + N_H{}^-(\theta)]. \quad (2)$$

In this formula, $N_H{}^+$ and $N_H{}^-$ are the K^+ counting rates per incident pion from free protons in each of the two opposite polarization states of the target (the positive sign denoting a spin orientation along the magnetic field direction). If the $KN\Sigma$ relative parity is assumed to be odd[5,6] then ϵ is related to that polarization P_Σ, which the Σ would have if produced from unpolarized protons, by the expression

$$P_\Sigma(\theta) = \epsilon(\theta)/P_T\langle\cos\phi\rangle_{\rm av}. \quad (3)$$

In this expression P_T is average target polarization and ϕ is the effective azimuthal angle for particles detected at angle θ.

As mentioned above, a π^- of momentum 1130 MeV/c in collision with a free proton can produce a K^+ only via reaction (1). Hence our positive identification of the K^+, which was made in the manner to be described below, guaranteed that reaction (1) had occurred. However, the LMN target contained only 3% by weight of hydrogen, and it was necessary to distinguish the desired free-proton events from the large background of K^+ mesons produced on protons bound in the heavier nuclei of target crystals. The usual constraints imposed by coplanarity and the angular correlation between the incoming and the two outgoing particles could not be used to make this distinction because almost all the Σ^- hyperons decayed before emerging from the target. Fortunately the Fermi motion of the bound protons leads to a nonunique value of the K^+ momentum at a given angle and this effect is particularly pronounced near the ΣK threshold. Thus it is possible to make a preferential selection of events from free protons by a rough range determination. The Lorentz transformation of reaction (1) implies that at each laboratory angle there are two possible K^+ momenta. Only the higher of these was observed in this experiment, the lower having always

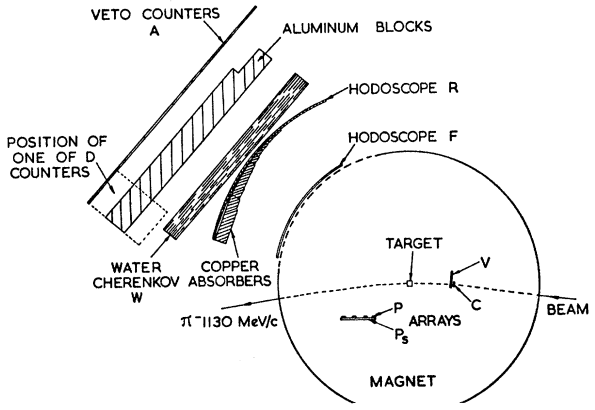

FIG. 2. Arrangement of counters around the target.

insufficient range to be detected. This caused our angular limit of $\cos\theta_\Sigma < +0.3$.

By these means the ratio of $\Sigma^- K^+$ events from bound protons to those from free protons was reduced to 3.5:1, from the gravimetric bound to free ratio of 15:1. This background was measured accurately by using a "dummy" target, lacking hydrogen but otherwise simulating the LMN target. It was made by sintering barium carbonate, magnesium oxide, and Teflon powder (polytetrafluorethylene) to give the same average atomic weight, ratio of heavy-to-light elements, and stopping power as the LMN crystals. The dummy and the LMN were aligned with the help of x radiography to within ± 0.8 mm of the same position.

The incident beam passed through four counter arrays. At the first focus $F1$ were two counters B_1 defining a momentum bite of 2.1% full width, and a gas Cherenkov counter G containing $CClF_3$ at a pressure of 65 lb/in.^{2} to veto electrons. Upstream of the polarized target was a beam hodoscope B_2 of eight horizontal strip counters whose main function was to help reject events in which more than one beam particle occurred during the counter resolution time. Finally, a square counter C of side 2.54 cm was placed immediately in front of and covering the target. It was surrounded by a veto counter V. Because of the size of the beam at $F2$ only 50% of the pions intercepted the LMN target.

The arrangement of counters around the target is shown in Fig. 2. The production angle of the K^+ was determined by two arrays F and R, each of 25 scintillation counters. A water Cherenkov counter W, viewed by seven phototubes, was placed behind array R to veto events with an outgoing charged particle of velocity $>0.75c$ (c is the velocity of light). All the elastically scattered pions and the great majority of elastic protons were thus rejected, with an efficiency of greater than 98% for particles of velocity $\sim c$. Copper degrader was placed between F and R so that the velocity of those K^+ mesons produced on free protons was reduced to $<0.6c$ and they stopped near the center of a thick aluminum block placed behind the water counter. Scintillation counters (labelled A) behind this block vetoed events in which the particle did not stop. The K^+ mesons thus decayed at rest with a mean life of 12.3 nsec and their charged decay products were detected in large scintillation counters D placed, in pairs, both above and below the aluminum. The members of each pair were separated by a 1.6-mm-thick brass sheet to ensure that only relatively energetic particles were counted. A K^+ meson therefore had the signature (Beam) $FR\bar{W}\bar{A}D$, where (Beam) was the sequence $B_1\bar{G}B_2C\bar{V}$, and the timing distribution of the D pulse was required to be consistent with the K^+ lifetime.

This technique for identifying a K^+ meson was similar in principle to that first used by Cool *et al.*[9] These authors detected Cherenkov light from the (relativistic) decay products, mainly from $K_{\mu 2}$ decay; in our case, however, the high noise rate of Cherenkov detectors together with the large background of charged particles scattered into our system would have given an unacceptably high rate of random coincidences. We therefore adopted our "passive" technique using only scintillation counters to detect the decay products. The loss in solid angle for detection was partially compensated by our ability to detect decay modes of the K^+ other than $K_{\mu 2}$.

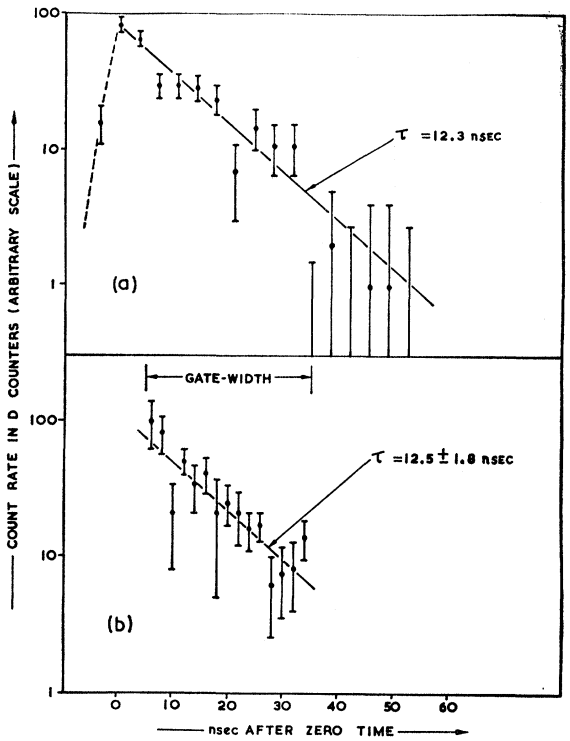

FIG. 3. Plots of logarithm of count rate against time, for pulses from D counters. (a) Distribution obtained under test conditions in a beam of positive particles; the line has the slope expected for K^+ mesons. (b) Typical distribution obtained in the experiment; the best-fits results with $\tau = 12.5 \pm 1.8$ nsec and zero background.

This system was tested prior to the experiment in a direct beam of positive particles from Nimrod of momentum 700 MeV/c, which contained about one K^+ per 2000 π^+. The K^+ mesons, having been selected preferentially by time of flight between B_1 and C, were first degraded to ≈ 350 MeV/c in lead and then stopped in the aluminum. Figure 3(a) shows the time distribution of D counter pulses obtained, plotted against the logarithm of the number of counts in each time channel. Figure 3(b) shows a typical time distribution obtained during the experiment. In each case the full lines were derived from a least-squares fit to an exponential decay law plus a constant background. Though the statistical accuracy of each point is low, the derived exponents are satisfactorily consistent with the lifetime of the K^+ meson.

[9] R. L. Cool, B. Cork, J. W. Cronin, and W. A. Wenzel, Phys. Rev. 114, 912 (1959).

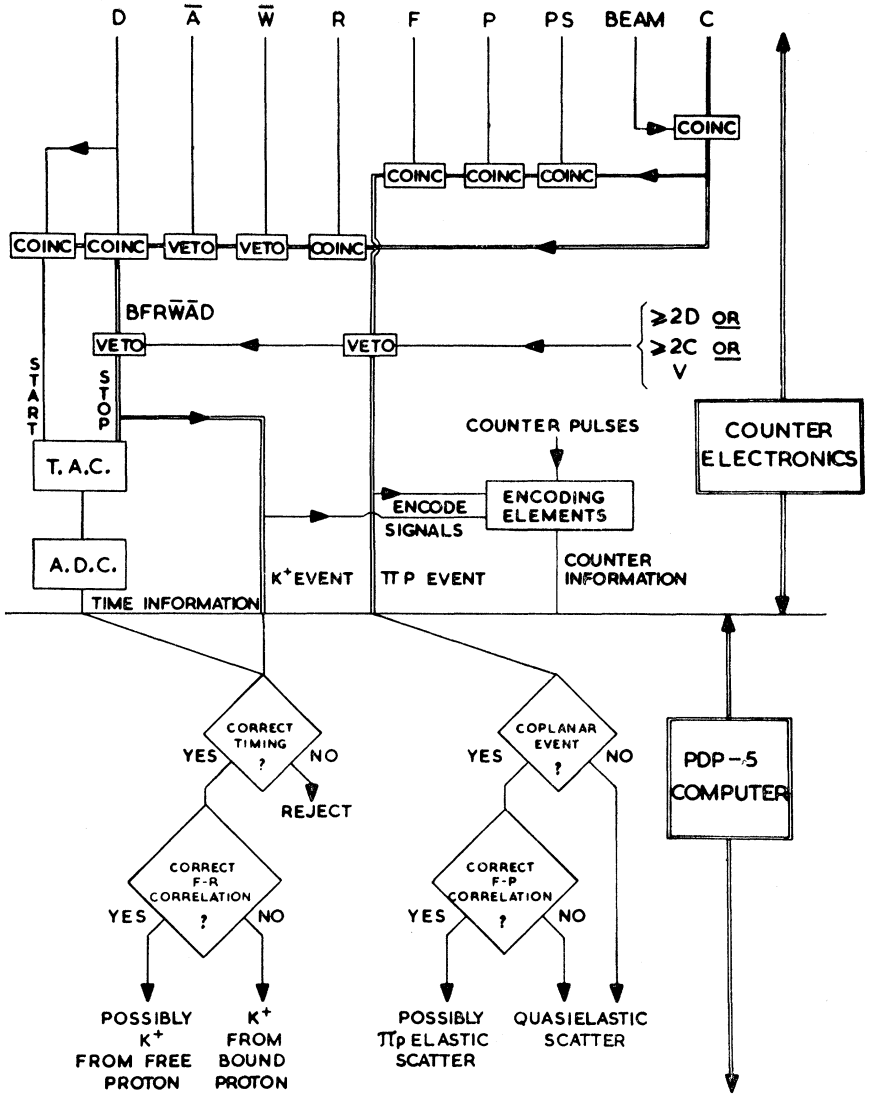

FIG. 4. Flow diagram of data-reduction system. Heavy lines show path of "strobe" pulse through system.

Throughout the experiment we also counted $\pi^- p$ scattering events, both elastic (from free protons) and quasi-elastic (from bound protons). Their signature was the sequence (Beam) FP where the π^- passed through one of the F counters and the recoil proton through one of the four P counters on the side of the target opposite the K^+ array. Information from three horizontal strip counters PS, behind the P counters, was used to identify coplanar events and hence deduce the ratio of elastic to quasi-elastic scatters. The quasi-elastic events being independent of target polarization monitored the beam intensity, and the angular asymmetry of the elastic events was used as a check on the target polarization; this is discussed further in Sec. III.

The electronic system chosen to process the counter pulses was designed around logic elements containing tunnel diodes as their active switches. These elements have the advantages of speed, flexibility, small size and power consumption and relatively low cost, important considerations since over 100 counters were used. Figure 4 is a block diagram of the logic involved. The system required a timing pulse, in this case from counter C, to be present for each event; all times were measured relative to this "strobe" which passed through a series of gates opened by the other counter pulses. Electronic timing jitter was thus reduced to a few tenths of a nanosecond. This was important because of the inevitable presence, in the time distribution of pulses from the D counters, of a large number of spurious events over and above the K^+ meson distribution, occurring at zero time. This "zero-time spike" amounted to as much as 50 times the total K^+ rate. This meant that events which appeared on the time distribution within 6 nsec of zero time had to be rejected when processing the data. The timing was done by means of a Harwell "2000" series time-to-amplitude converter

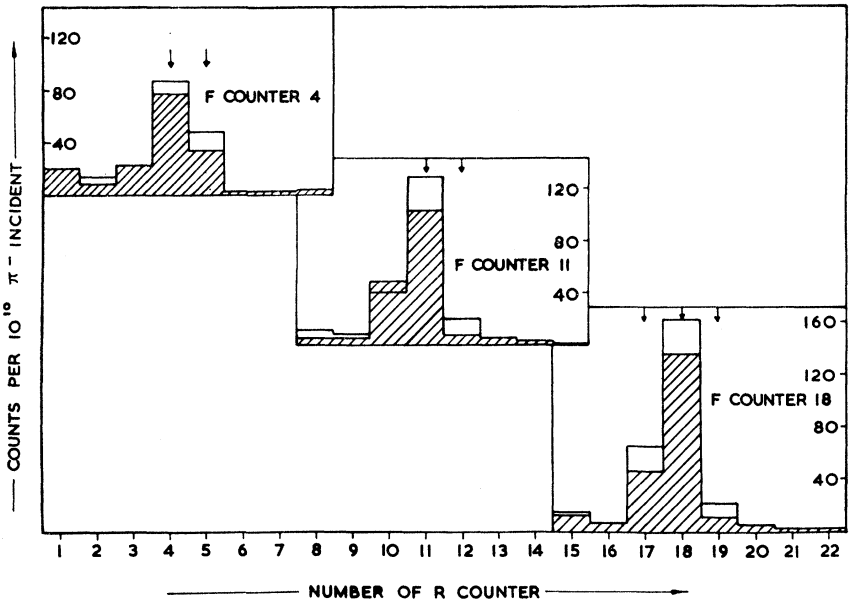

FIG. 5. Histograms showing the count rates in various R counters, for three of the F counters. Open histograms denote counts from the LMN target; hatching denotes counts from the dummy target. Those hydrogen-effect pairings selected by the Monte Carlo program are indicated by arrows.

followed by an analog-to-digital converter (ADC) operating over 128 channels. Frequent checks of the calibration were made. The degree of linearity was measured by placing known lengths of cable between "start" and "stop" pulses, and the channel uniformity checked by using "stop" pulses derived from randomly occurring cosmic-ray counts.

Events were recorded as digital information in a PDP-5 computer connected on line to the electronic system. The computer was used both as a diagnostic aid, displaying histograms of counter and timing information during the experiment, and as a preprocessor of data, dividing up events by applying simple selection criteria. A K^+ event was processed as follows (see Fig. 4): The timing information from the ADC was interrogated and the event accepted only if the delay between the strobe pulse C and the pulse from the decay counter D lay between preselected limits. Thus, events in the zero-time spike, and those with decay delay greater than approximately 30 nsec were rejected (though the information was retained for diagnostic purposes). Also, the F-R correlation of good events was determined. K^+ mesons produced on free protons at a point target would have had unique trajectories in the magnetic field and would thus have passed through a unique pair of array counters. In practice, finite target size and energy loss smeared this correlation so that the so-called "effect" channels were spread over about three R counters for a given F. Such correlations were far weaker for K^+ mesons produced on bound protons possessing Fermi momenta, and this was a second way (preferential range selection being the first) of enhancing the free-to-bound ratio of K^+.

$\pi^- p$ scattering events were processed by recording the F-P counter correlation. Checks as to whether the events were coplanar with the incident-beam direction enabled a preliminary separation of elastic and quasi-elastic events to be made.

Counter information for each event was held in a buffer store during the synchrotron spill-time. Between bursts, this information was used to increment various multiscaler locations in the core store, each location representing a particular F-R pair (for K^+ events) or F-P-PS correlation (for πp events). At the end of each experimental run the contents of these locations together with information on run conditions were punched onto paper tape for subsequent analysis using the IBM 360/75 computer at this laboratory.

To reduce the effect of time-varying conditions, runs were performed with the following sequence of target conditions: positive polarization ($+P_T$), negative polarization ($-P_T$), dummy target, $-P_T$, and $+P_T$. A run under each condition lasted about four hours and contained about 2×10^9 incident pions. Each such series of runs constituted a "cycle" and ten cycles of data were taken. Our event rate was limited both by the size of the PDP-5 buffer store and by the necessity of rejecting events in which more than one beam particle was registered during the D counter time gate. These limits restricted our incident beam to about 3×10^5 π^- per pulse.

III. DATA ANALYSIS AND RESULTS

The analysis proceeded in two steps, the extraction of count rates due to free protons in the target, and the calculation of polarizations. A Monte Carlo program, originally written to assist in the design stage, was used to generate K^+ events at random positions in the target and helped in calculating the relevant counter correlations and angles.

TABLE I. Angular asymmetries for the reaction $\pi^- p \to \Sigma^- K^+$ at 1130 MeV/c and the corresponding polarization of the Σ^-.

$\langle\cos\theta_\Sigma\rangle_{av}$	rms range of $\cos\theta_\Sigma$	$\langle\cos\phi_\Sigma\rangle_{av}$	rms range of $\cos\phi_\Sigma$	Asymmetry ϵ	Polarization of Σ^- p_Σ[a]
−1.000	±0.019	0.035	±0.877	+0.065±0.088	(3.71 ±5.03)
−0.968	±0.025	0.774	±0.228	−0.167±0.094	−0.431±0.242
−0.903	±0.046	0.946	±0.055	−0.112±0.094	−0.236±0.198
−0.784	±0.075	0.974	±0.026	−0.061±0.088	−0.125±0.180
−0.639	±0.096	0.987	±0.014	−0.055±0.098	−0.111±0.198
−0.435	±0.124	0.992	±0.010	−0.123±0.103	−0.247±0.207
−0.184	±0.159	0.994	±0.007	−0.188±0.090	−0.378±0.181
+0.128	±0.165	0.996	±0.006	−0.220±0.087	−0.440±0.174

[a] Absolute normalization error of ± 16% is *not* included.

For a run under given target conditions the K^+ information was contained in a single F-R correlation matrix, and a time distribution of decays. Had the LMN and dummy targets been identical apart from their hydrogen content, a simple subtraction would have given the over-all rate from free protons:

$$(N_H)_{ij} = (N)_{ij} - \eta(N_D)_{ij},$$

where N_H, N, and N_D are the normalized rates from free protons, LMN target, and dummy target, respectively; i and j refer to the counter positions in the F and R arrays; and η is unity.

It was found that taking $\eta = 1$ did *not* give a zero value of N_H in all F-R combinations outside those expected to show an effect from free hydrogen. Evidently the LMN and dummy targets differed to a small but significant extent in their effective content of bound protons. To determine the best value of η we used the Monte Carlo program to select those F-R combinations through which K^+ mesons from free protons could pass. We then demanded that the summed values of N_H, for values of i, j other than those pairings, be zero, i.e.,

$$\sum_{i,j}(N_H)_{ij} = 0$$

summing over all i, j pairs except hydrogen-effect combinations. This procedure gave a value of

$$\eta = 1.0609 \pm 0.0274.$$

We show in Fig. 5 some typical histograms of count rates for various F-R combinations, together with the hydrogen-effect pairings selected by the Monte Carlo program. It is evident that in most cases the same selection could have been been made by inspection.

For further analysis the 25 F counters were grouped into eight roughly equal angular bins. For each bin the asymmetry $\epsilon(\theta)$ was evaluated. The appropriate polar and azimuthal angles θ and ϕ were derived from the Monte Carlo program, assuming equal weight for each F counter in the group. Thus, for each angular bin a range of values of θ and ϕ was generated. In Table I we give the average values of $\cos\theta$ and $\cos\phi$ for each bin, and their rms ranges about these values. The program was run a sufficient number of times for the standard errors of the means to be negligible. The Σ^- polarizations were then calculated from Eq. (3) and are given in Table I and Fig. 6. This figure shows also the measurement made by Weldon *et al.*[1] at 1145 MeV/c, which is in good agreement with our results. We have calculated the average value of P_Σ for each of our ten cycles of data taking. These values are given in Table II and give no cause to doubt our internal consistency.

The quoted errors on P_Σ include only the standard statistical errors on ϵ; they do not include the absolute normalization error of ±16% on the target polarization. The large error on ϵ at $\cos\theta_\Sigma = 1$ renders useless any comparison between the experimental value of P_Σ for the first angular bin, and its necessary value of zero at this angle.

The analysis of $\pi^- p$ events proceeded as shown in Fig. 4. Elastic events were selected by requiring, first, that the protons pass through the central one of the three strip counters PS, and thus be coplanar with the incoming and outgoing π^-, and, second, that the event have the correct F-P counter correlation to satisfy elastic kinematics. The remaining quasi-elastic events were detected only in the dummy target runs, and subtracted out. The elastic $\pi^- p$ asymmetries and polarizations were then evaluated in the angular regions defined by the four P counters, using the same mean target polarization as before. The results are compared in Fig. 7 with those derived by interpolation between previous measurements[10] in this energy region. Though the errors

TABLE II. Average values of the Σ^- polarization for each cycle of data taking, and the over-all average value.

Cycle No.	Polarization p_Σ[a]
1	−0.61±0.61
2	−0.59±0.32
3	−0.40±0.33
4	−0.27±0.26
5	−0.19±0.28
6	−0.70±0.66
7	+0.16±0.27
8	−0.13±0.27
9	−0.31±0.17
10	+0.02±0.23
Over-all average polarization	−0.22±0.09

[a] Absolute normalization error of ± 16% is *not* included.

[10] P. J. Duke, D. P. Jones, M. A. R. Kemp, P. G. Murphy, J. J. Thresher, H. H. Atkinson, C. R. Cox, and K. S. Heard, Phys. Rev. **166**, 1448 (1968).

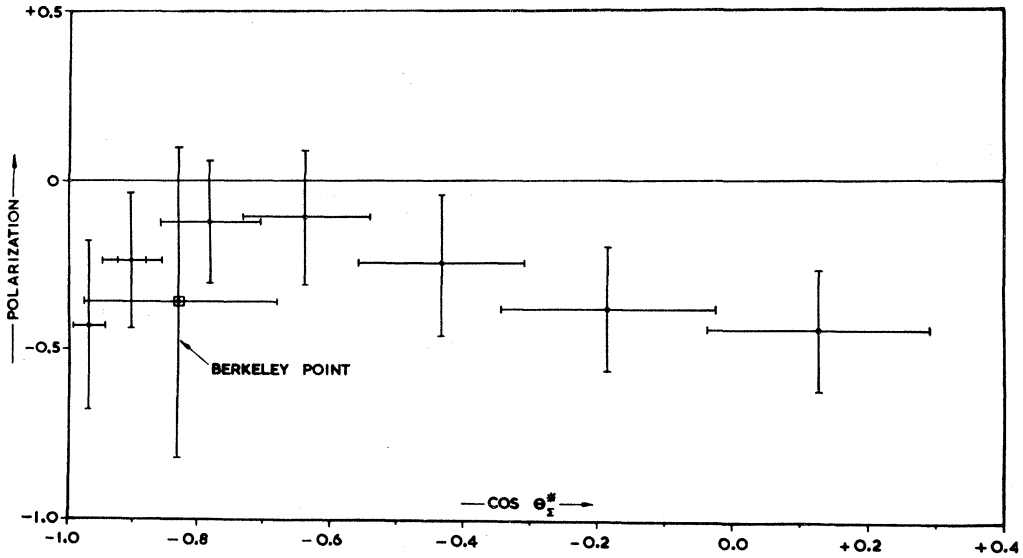

FIG. 6. Values of Σ^- polarization determined in this experiment, showing also the measurement of Weldon *et al.* (Ref. 1). There is an additional absolute normalization error of $\pm 16\%$.

are large the agreement gives us confidence in our measurement of the Σ^- polarization.

IV. PARTIAL-WAVE ANALYSIS

The reaction

$$\pi+p\rightarrow\Sigma+K \tag{4}$$

may be described by a 2×2 matrix M:

$$M=f(\theta)+i\hat{\sigma}\cdot\hat{n}g(\theta).$$

Here $\hat{\sigma}$ is the Pauli spin operator and $\hat{n}$ is the unit vector $\mathbf{k}_\pi\times\mathbf{k}_\Sigma/|\mathbf{k}_\pi\times\mathbf{k}_\Sigma|$. The cross sections and polarizations can be written as

$$d\sigma/d\Omega=|f(\theta)|^2+|g(\theta)|^2, \tag{5}$$

and

$$P(d\sigma/d\Omega)=-2\,\mathrm{Im}[f^*(\theta)g(\theta)]. \tag{6}$$

The amplitudes $f(\theta)$ and $g(\theta)$, for non-spin-flip and spin-flip transitions, respectively, can be expanded in terms of partial-wave amplitudes $A_{l\pm}$, for total angular momentum $j=l\pm\frac{1}{2}$:

$$f(\theta)=\sum_l[(l+1)A_{l+}+lA_{l-}]P_l(\cos\theta),$$

and

$$g(\theta)=\sum_l[A_{l+}-A_{l-}]P_l^1(\cos\theta), \tag{7}$$

where P_l, P_l^1 are the Legendre and first associated Legendre polynomials of order l, respectively.

By the hypothesis of charge independence the amplitudes for the three isospin channels $\pi^+p\rightarrow\Sigma^+K^+$, $\pi^-p\rightarrow\Sigma^-K^+$, and $\pi^-p\rightarrow\Sigma^0K^0$ may be written in terms of $I=\frac{1}{2}$ and $I=\frac{3}{2}$ amplitudes as

$$A^+=A_{3/2},$$
$$A^-=\tfrac{1}{3}(A_{3/2}+2A_{1/2}),$$

and

$$A^0=(\tfrac{1}{3}\sqrt{2})(A_{3/2}-A_{1/2}), \tag{8}$$

respectively. [Equations (8) hold separately for each partial-wave amplitude $A_{l\pm}$, the angular momentum indices being suppressed for clarity.] Using Eqs. (5)–(8) one may hope to determine the $I=\frac{1}{2}$ and $I=\frac{3}{2}$ amplitudes from the differential cross sections and polarizations in the three channels of reaction (4).

Because of the angular-momentum barrier, it is reasonable to assume that only the lower partial waves will contribute near threshold. The best fit to the data will fix the maximum number of terms in Eq. (7), and hence the maximum partial wave l required. On the other hand, if πN resonances of high spin are present in the direct channel they may, even if not strongly coupled to the ΣK system, interfere with lower angular-momentum states and complicate the analysis.

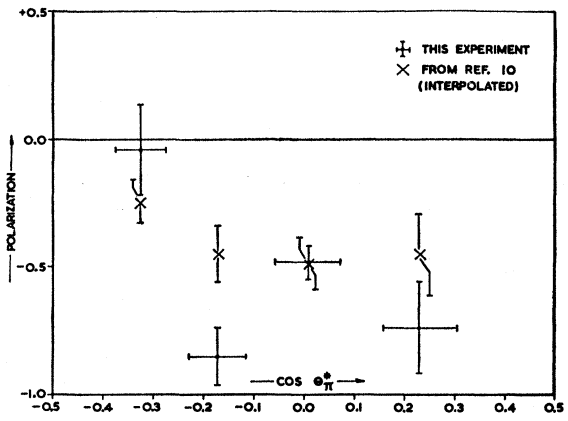

FIG. 7. Values of the polarization in π^-p elastic scattering.

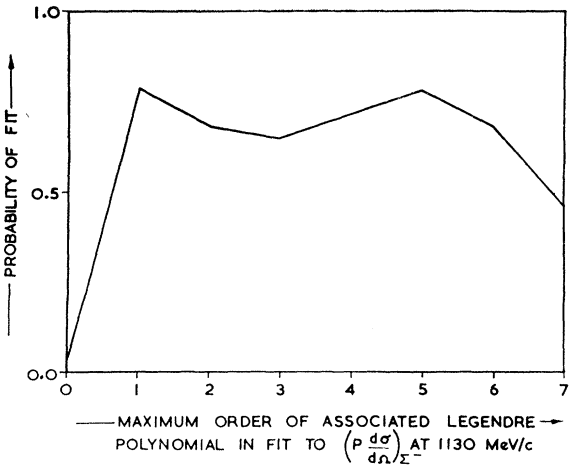

FIG. 8. The χ^2 probability of a fit of the form $(Pd\sigma/d\Omega)_{\Sigma^-}=\sum_{n=0}^{N} D_n P_n^1(\cos\theta_\Sigma)$ to the data at 1130 MeV/c, for various values of N.

An energy-independent partial-wave analysis of our data was unlikely to be fruitful, because of the sparse information on $\pi p \to \Sigma K$ at the same incident momentum as in this experiment. We have therefore carried out an energy-dependent analysis for reaction (4) between threshold and 1170 MeV/c. We have expressed the partial-wave amplitudes in the form

$$A_n = a_n e^{i\psi_n} k_\Sigma^{(l+1/2)}, \tag{9}$$

where k_Σ is the c.m. momentum of the Σ, the parameters a_n and ψ_n are real, and the index n labels isotopic spin, total spin, and parity of the amplitude. The phase convention is such that the $I=\frac{3}{2}$, S-wave amplitude is real and positive. This form for the amplitudes, strictly valid only near threshold, was suggested by Lee *et al.*[11] and has been used previously[12] to determine the $I=\frac{3}{2}$ amplitudes from the reaction $\pi^+ p \to \Sigma^+ K^+$.

It is well known that measurements of differential cross sections and polarization angular distributions do not determine uniquely the partial-wave amplitudes. In particular, it can be shown by substitution that these quantities, given by Eqs. (5) and (6) are invariant under the following generalization of the Yang transformation:

$$A_{l+}{}^T = \pm(2l+1)^{-1}[A_{l+}{}^* + 2lA_{l-}{}^*],$$
$$A_{l-}{}^T = \pm(2l+1)^{-1}[2(l+1)A_{l+}{}^* - A_{l-}{}^*]. \tag{10}$$

Here $A_{l\pm}{}^T$ are the transformed amplitudes, and $A_{l\pm}{}^*$ are the complex conjugates of the normal amplitudes.[13]

The form of Eq. (9) obviously gives the same energy-dependence for amplitudes with the same l value but different total spin; therefore, the solutions obtained in this analysis suffer from the Yang ambiguity of Eq. (10). On the other hand, the different energy dependence assumed for partial waves of the same total spin but different l values eliminates the generalized Minami ambiguity.[14]

The data used in the analysis contained differential cross sections[2–4,12,15–20] and polarizations[1,3,4,16,21] for all three channels of reaction (4). The total number of data points for each channel was 56 for $\pi^+ p \to \Sigma^+ K^+$, 36 for $\pi^- p \to \Sigma^- K^+$, and 32 for $\pi^- p \to \Sigma^0 K^0$. We first determined the maximum order of partial wave needed to fit $P(d\sigma/d\Omega)_{\Sigma^-}$ near 1130 MeV/c, using our values of P_{Σ^-} and the cross sections at 1128 MeV/c from Ref. 19. The probability of a fit for various numbers of terms in the associated Legendre series expansion of $P(d\sigma/d\Omega)_{\Sigma^-}$ is shown in Fig. 8. Evidently only S and P partial waves are required, as increasing the order beyond $N=1$ does not improve the fit. The analysis was therefore confined to S and P waves (11 free parameters) for the data below 1130 MeV/c. However, S, P, and D waves (19 free parameters) were used for the complete data set, in accordance with previous Legendre polynomial fits to the data at the higher momenta.[2–4]

The analysis consisted in varying the parameters so as to minimize the quantity

$$\mathfrak{M} = \sum_i (x_i - X_i)^2/\Delta x_i,$$

where x_i are the experimental values, Δx_i are their corresponding variances, and X_i are the values calculated from the partial-wave amplitudes. The computer program VA04A was used to adjust the parameters and minimize $\mathfrak{M}$. We found this program to be more efficient than MINFUN for our purposes. However MINFUN was used to carry out an error analysis of the minimized solutions.

The random-starting-point method was used in an attempt to find all the partial-wave solutions. In prin-

[11] T. D. Lee, J. Steinberger, G. Feinberg, P. K. Kabir, and C. N. Yang, Phys. Rev. **106**, 1367 (1957).

[12] F. Grard and G. A. Smith, Phys. Rev. **127**, 607 (1962).

[13] It is interesting to observe that the requirement of unitarity, which in the case of elastic scattering compels the transformed amplitudes to lie *on* the unitarity circle, is much weaker in inelastic processes. In these the only restriction is that the transformed amplitudes lie *within* the unitarity circle, and this condition is sure to be satisfied in practice for channels with low branching ratios. In such cases the transformation of *amplitudes* [Eq. (10)] may safely be used, in place of the similar, but approximate, relation between *phase shifts*.

[14] M. Nauenberg and A. Pais, Phys. Rev. **123**, 1058 (1961).

[15] C. Balty, H. Courant, W. J. Fickinger, E. C. Fowler, H. L. Kraybill, J. Sandweiss, J. R. Sanford, D. L. Stonehill, and H. D. Taft, Rev. Mod. Phys. **33**, 374 (1961).

[16] N. L. Carayannopoulos, G. W. Tautfest, and R. B. Willmann, Phys. Rev. **138**, B433 (1965).

[17] F. Eisler *et al.*, Nuovo Cimento **10**, 468 (1958).

[18] F. S. Crawford, Jr., M. Cresti, M. L. Good, K. Gottstein, E. M. Lyman, F. T. Solmitz, M. L. Stevenson, and H. K. Ticho, reported by J. Steinberger in *Proceedings of the 1958 CERN Conference on High-Energy and Elementary-Particle Physics* (CERN Scientific Information Service, Geneva, 1958), p. 147.

[19] R. R. Kofler, thesis, University of Wisconsin, 1964 (unpublished); M. L. Good and R. R. Kofler, University of Wisconsin Report, 1965 (unpublished).

[20] T. O. Binford, thesis, University of Wisconsin, 1965 (unpublished).

[21] Y. S. Kim, G. R. Burleson, P. I. P. Kalmus, A. Roberts, C. L. Sandler, and T. A. Romanowski, Phys. Rev. **151**, 1090 (1966).

ciple this method consists in making a large number of minimizations from random initial values of the parameters. The procedure is continued until it appears that no more solutions with acceptable $\mathfrak{M}$ values are likely to be found. In our case this method was too time consuming on the computer so the following procedure was adopted. The program MINFUN was run from a small number of random starting points in its "positive step" mode in order to find suitable starting points for minimizations. The program VAO4A was then used to perform the minimizations from these selected starting points. In the case of the *SP* analysis a number of independent random starting points were also used in the minimizations. The total number of starting points in the *SP* analysis was 93, of which 36 were obtained from the MINFUN searches and 57 were independent sets of random starting values. In the case of the *SPD* analysis the total number of starting points was 11. In addition, all *S*- and *P*-wave solutions were used as starting values for *SPD* minimizations.

Four *S* and *P* solutions with acceptable $\mathfrak{M}$ values were found in the search between threshold and 1130 MeV/*c*. These $\mathfrak{M}$ values (identical, at their minima, with χ^2) were all close to the expected value of 55. Table III gives both the regular solutions and those obtained by the generalized Yang transformation [Eq. (10)]. The χ^2 contributions of each data set are given in Table IV and the error matrix for a typical regular solution is given in Table V. The results of the *SPD* search over the full data set are also given in Tables III and IV. Only one *SPD* solution was found with an acceptable $\mathfrak{M}$ value (153 compared with the expected value of 105). The probability of this solution's fitting the data is $\approx 5\%$.

From Table III it can be seen that corresponding $I=\frac{3}{2}$ amplitudes in the four *SP* solutions are consistent with one another. The amplitudes also agree well with the $I=\frac{3}{2}$ *S*- and *P*-wave amplitudes in the single *SPD* solution. The $\pi^+p\to\Sigma^+K^+$ data are well fitted at all incident momenta. We therefore conclude that the $I=\frac{3}{2}$ amplitudes are uniquely determined (apart from the generalized Yang ambiguity) and that the use of Eq. (9) for these amplitudes is justified up to 1170 MeV/*c*.

The situation concerning the $I=\frac{1}{2}$ amplitudes is less clear. The four *SP* solutions found at low energy have distinctly different values of $I=\frac{1}{2}$ parameters. The full data set used for the *SPD* analysis does not appear to support the form of Eq. (9) for these amplitudes. The point is best illustrated by comparing the χ^2 contributions of the pure $I=\frac{3}{2}$ data with the data involving a mixture of isospin states. In the *SPD* solution the former ($\pi^+p\to\Sigma^+K^+$) contributes 52 to the total χ^2, for 56 data points, whereas the latter ($\pi^-p\to\Sigma^-K^+$ and Σ^0K^0) contributes 101 to the χ^2, for 68 data points. The fact that some acceptable $\mathfrak{M}$ values were obtained using *S* and *P* waves only does suggest that the energy dependence expressed by Eq. (9) is adequate below 1130

TABLE III. The amplitudes found by the partial wave analysis of reaction $\pi p\to\Sigma K$ between threshold and 1170 MeV/*c*. The parameters a_n and ψ_n are defined by Eq. (9). We list the four solutions found for *S* and *P* waves only, and the single solution for *S*, *P*, and *D* waves. The polarizations and cross sections are invariant under the transformation of Eq. (10) which produces the "Yang" solutions listed. Units of a_n are $[\text{mb/sr}]^{1/2}[\text{GeV}/c]^{-(l+1/2)}$; units of ψ are radians.

	SP1		*SP2*		*SP3*		*SP4*		*SPD*	
L_{IJ}	Regular	Yang	Regular	Yang	Regular	Yang	Regular	Yang	Regular	Yang
S_{31} a	0.195±0.010	0.195±0.010	0.201±0.010	0.201±0.010	0.191±0.011	0.191±0.011	0.202±0.008	0.202±0.008	0.199±0.007	0.199±0.007
ψ	0.0	0.0	0.0	0.0	0.0	0.0	0.0	0.0	0.0	0.0
S_{11} a	0.028±0.018	0.028±0.018	0.208±0.026	0.208±0.026	0.427±0.015	0.427±0.015	0.442±0.014	0.442±0.014	0.464±0.007	0.464±0.007
ψ	3.804±0.652	2.479±0.652	3.316±0.109	2.968±0.109	2.097±0.106	4.186±0.106	3.784±0.103	2.499±0.103	2.151±0.081	4.132±0.081
P_{31} a	0.725±0.093	0.096±0.120	0.666±0.107	0.088±0.080	0.737±0.106	0.073±0.126	0.616±0.106	0.137±0.124	0.533±0.079	0.180±0.081
ψ	0.919±0.172	0.124±0.745	0.776±0.152	5.179±1.057	0.905±0.176	5.820±1.376	0.955±0.201	0.018±0.601	0.916±0.140	0.301±0.358
P_{33} a	0.226±0.054	0.556±0.057	0.230±0.050	0.521±0.060	0.235±0.054	0.569±0.066	0.228±0.059	0.482±0.065	0.220±0.045	0.417±0.049
ψ	0.639±0.272	5.402±0.116	0.869±0.241	5.493±0.099	0.805±0.274	5.392±0.120	0.573±0.288	5.387±0.132	0.303±0.183	5.468±0.096
P_{11} a	2.717±0.052	0.299±0.074	0.434±0.169	2.406±0.077	0.829±0.137	1.069±0.121	0.673±0.107	1.103±0.112	0.073±0.122	0.244±0.109
ψ	4.586±0.145	4.614±0.526	3.130±0.252	1.308±0.170	3.723±0.209	2.869±0.222	5.123±0.296	0.918±0.225	0.746±1.243	3.068±0.432
P_{13} a	0.463±0.051	1.965±0.037	1.779±0.054	0.601±0.067	1.001±0.077	0.880±0.083	0.991±0.076	0.775±0.071	0.169±0.095	0.039±0.059
ψ	4.478±0.211	1.706±0.134	4.917±0.150	1.855±0.153	3.478±0.155	2.653±0.123	5.325±0.156	1.075±0.158	3.149±0.339	4.143±0.835
D_{33} a									0.611±0.236	0.530±0.193
ψ									3.764±0.319	0.915±0.365
D_{35} a									0.450±0.146	0.514±0.167
ψ									5.140±0.317	2.346±0.311
D_{13} a									1.148±0.354	0.507±0.350
ψ									1.433±0.326	3.511±0.431
D_{15} a									0.502±0.270	0.979±0.241
ψ									2.392±0.496	4.767±0.260
Total χ^2	52.34		53.56		51.91		51.51		153.44	

TABLE IV. Experimental data used in the partial wave analysis, listing the incident beam momentum and the contribution of each data set to the total value of χ^2.

	Reference	Momentum (MeV/c)	No. of data points	χ^2 contributions to solutions *SP1*	*SP2*	*SP3*	*SP4*	*SPD1*
$d\sigma/d\Omega$								
$\pi^+p\to\Sigma^+K^+$	12	1050	10	7.24	6.35	8.44	6.74	8.77
$\pi^-p\to\Sigma^-K^+$	17	1090	5	15.26	14.86	8.69	9.31	10.39
$\pi^+p\to\Sigma^+K^+$	15,16	1111	16	9.29	9.07	9.49	8.11	11.34
$\pi^-p\to\Sigma^-K^+$	18	1120	3	2.29	2.24	2.59	2.70	4.99
$\pi^-p\to\Sigma^-K^+$	19	1128	10	2.64	2.84	3.15	2.62	19.28
$\pi^-p\to\Sigma^0K^0$	20	1128	10	9.87	10.10	13.68	15.36	26.59
$\pi^-p\to\Sigma^0K^0$	4	1170	10					7.33
$\pi^-p\to\Sigma^-K^+$	2	1170	10					16.29
$\pi^+p\to\Sigma^+K^+$	3	1170	20					26.49
Polarization								
$\pi^+p\to\Sigma^+K^+$	16	1111	5	1.96	3.32	2.10	2.77	2.25
$\pi^-p\to\Sigma^-K^+$	this expt.	1130	7	3.79	4.78	3.77	3.90	5.01
$\pi^-p\to\Sigma^-K^+$	1	1145	1					0.48
$\pi^-p\to\Sigma^0K^0$	4,21	1170	12					12.91
$\pi^+p\to\Sigma^+K^+$	3	1170	5					1.33
			Total value of χ^2	52.34	53.56	51.91	51.51	153.44

TABLE V. Error matrix for solution *SP*1.

	S_{31}	S_{11}		P_{31}		P_{33}		P_{11}		P_{13}	
	a	a	ψ	a	ψ	a	ψ	a	ψ	a	ψ
S_{31} a	0.00009	0.00004	−0.00126	−0.00066	0.00053	0.00014	−0.00069	−0.00015	0.00016	0.00001	−0.00022
S_{11} a		0.00031	−0.00296	−0.00041	−0.00002	0.00000	−0.00003	−0.00003	−0.00022	0.00006	−0.00124
ψ			0.42512	0.01149	−0.01138	−0.00471	0.01271	0.00404	−0.04705	−0.00104	0.00470
P_{31} a				0.00866	−0.00867	−0.00274	0.01038	0.00146	−0.00179	−0.00035	0.00461
ψ					0.02973	0.00613	−0.03187	0.00043	0.00900	0.00004	−0.00788
P_{33} a						0.00291	−0.00505	−0.00026	0.00236	0.00048	−0.00202
ψ							0.07421	−0.00031	−0.00849	0.00222	0.01643
P_{11} a								0.00272	−0.00197	−0.00036	−0.00081
ψ									0.02107	0.00008	0.00331
P_{13} a										0.00263	−0.00193
ψ											0.04434

MeV/c. Furthermore, it has been noted[3] that any departure from this behavior is evidence for resonant behavior in the reaction channels. We note that the recent CERN phase-shift analysis[22] of the π-nucleon system does suggest that the P_{11} partial wave has a broad, highly inelastic resonance near an incident momentum of 1144 MeV/c. Inclusion of this resonance in our analysis might possibly improve the fit. However, the quantity of data giving information on the $I=\frac{1}{2}$ amplitudes is very limited at the lower energies. More data are needed to establish the range of validity of Eq. (9).

The analysis described here assumes that the principle of charge independence is valid for the three channels of reaction (4). Any violation in this reaction would result in an inability of the minimization program to produce a good fit to the data. A possible violation of charge independence in this reaction has been suggested[19] at 1125 MeV/c incident momentum, in the angular range $-1.0<\cos^*_2<-0.7$. The acceptable $\mathfrak{M}$ values obtained in the *SP* analysis indicate that this supposed violation is not statistically significant.

[22] C. A. Lovelace, *Proceedings of the Heidelberg International Conference on Elementary Particles* (North-Holland Publishing Co., Amsterdam, 1968), p. 79.